Physica A 392 (2013) 1232–1245

Contents lists available at SciVerse ScienceDirect

Physica A

journal homepage: www.elsevier.com/locate/physa

Analysis on the evolution process of BFW-like model with discontinuous percolation of multiple giant components

Renquan Zhang, Wei Wei *, Binghui Guo, Yang Zhang, Zhiming Zheng

LMIB and School of Mathematics and Systems Science, Beihang University, Beijing, 100191, PR China

ARTICLE INFO

Article history:
Received 12 August 2012
Received in revised form 26 October 2012
Available online 28 November 2012

Keywords:
Discontinuous percolation
BFW model
Multiple giant components
Evolution process

ABSTRACT

Recently, the modified BFW model on random graphs [W. Chen, R.M. D'Souza, Phys. Rev. Lett. 106 (2011) 115701], which shows a discontinuous percolation transition with multiple giant components, has attracted much attention from physicists and statisticians. In this paper, by establishing the evolution equations on the modified BFW model, the evolution process and steady-states on both random graphs and finite-dimensional lattices are analyzed. On a random graph, by varying the edge accepted rate α, the system stabilizes in a steady-state with different numbers of giant components. Moreover, a close correspondence is built between the values of α and the number of giant components in steady-states, the efficiency of which is verified by the numerical simulations. Then, the sizes of giant components for different evolution strategies can be obtained by solving some constraints derived from the evolution equations. Meanwhile, a similar analysis is expanded to finite-dimensional lattices, and we find the BFW (α) model on a finite-dimensional lattice has different steady-states from those on a random graph, but they have the same evolution mechanism. The analysis of the evolution process and steady-state is of great help to explain the properties of discontinuous percolation and the role of nonlocality.

1. Introduction

Percolation is a classical model in statistical physics, probability theory, complex networks and epidemiology, which is initiated as a mathematical framework for the study of random physical processes such as flow through a disordered porous medium [1,2]. The research in percolation is not only of academic interest but also of considerable practical value. During the last five decades, percolation theory has found a broad range of application in epidemic spreading, porous media, robustness of networks to attacks [3–5], etc.

Percolation has been studied on various topological structures such as scale-free networks, lattices with different dimensions, random graphs, etc. Taking a percolation model on the Erdös–Rényi random graph (ER model) as an example, this model is one of the most simple and classical models that undergoes a phase transition of an emerging giant component. Typically, the percolation phase transition is considered as a robust second-order transition until recent work by Achlioptas, et al. [6], in which they propose that the phase transition of some certain Achlioptas process is discontinuous, and call it *explosive percolation*. This interesting phenomenon leads to intensive studies [7,8] on the other models like scale-free networks [9,10], local cluster aggregation models [11], lattices [12,13], etc. More recently, it has been demonstrated that all Achlioptas processes have continuous phase transitions in the mean-field limit [14–19]. But some other kinds of models, which have different and special rules of evolution [20–27], such as the triangle rule [11] and largest cluster rule [28], have been analyzed in detail and indeed exhibit explosive percolation.

* Corresponding author.
E-mail address: weiw@buaa.edu.cn (W. Wei).

0378-4371/$ – see front matter
doi:10.1016/j.physa.2012.11.033

In particular, the BFW model on random graphs, originally introduced by Bohman, Frieze, and Wormald [29], is similar to Achlioptas processes but more restricted. The recent work of W. Chen and R. M. D'Souza [30,31], shows a discontinuous percolation with multiple giant components in the BFW model. It is also shown that with smaller values of edge accepted rate α, the transition will become more *explosive* and the number of giant components will increase. Furthermore, K. J. Schrenk et al. [32] generalize the results to the lattice with different dimensions.

So far, although continuous percolations on several topological structures have been analyzed theoretically and a wealth of rigorous results have been obtained, such as one- and two-dimensional percolations [33,34], and mean-field percolation [35], the discontinuous ones still remain on research, especially the BFW model. Many properties of the BFW model are still not clear, which drives us to investigate the evolution process of the BFW model with both simulation and theoretical methods.

This paper is organized as follows. In Section 2, we introduce the BFW algorithm with parameter α in detail; the mathematical expression of the BFW model is established and analyzed in theory. In Section 3, the dynamical evolution equations of the BFW (α) model on random graphs are described accurately, by which we obtain the steady-state condition and evolution mechanism of the BFW model for any α; meanwhile, we find the relationship between parameter α and the steady-state, that is when $\alpha \in (\frac{1}{m+1}, \frac{1}{m}]$, the BFW algorithm must stabilize with m giant components, for any $m \in \mathbb{N}^+$; moreover, the sizes of these components must satisfy some constraint equations which are given in our paper. In Section 4, the evolution equations and steady-state of the BFW (α) model are expanded to the finite-dimensional lattice; comparing to the random graph, we find some *metastable states* during the evolution process, which are similar to the steady-states on random graphs. In Section 5, we give a brief discussion about the scaling properties and nonlocality; based on the analysis above, we can prove the transition of the BFW (α) model is discontinuous by both theoretical methods and simulations.

2. Evolution analysis on the BFW (α) model

The BFW model on random graphs is first introduced by T. Bohman, A. Frieze, and N. C. Wormald [29], aiming to choose a subset $A \subset \{e_1, e_2, \ldots, e_{2t}\}$ with $|A| = t$ such that for t as large as possible the size of the largest component in $G = (n, A)$ is $o(n)$ (i.e. G does not contain a giant component); here n denotes the number of nodes and $\{e_1, e_2, \ldots\}$ are the sequence of edges chosen randomly and uniformly from the edge set of the complete graph; A represents the set of accepted edges (initialized to $A = \emptyset$) and $t = |A|$ represents the number of accepted edges.

According to the BFW model, one of the sampled edges is considered at each step, and either accepted to the graph or rejected provided that the fraction of accepted edges is never smaller than the decreasing function $g(k)$, which asymptotically approaches the value $1/2$. If taking u as the total number of sampled edges, the fraction of accepted edges is represented by t/u; k denotes the stage and the function $g(k) = 1/2 + 1/\sqrt{2k}$. Just similar to the Achlioptas process, in which half of the sampled edges are accepted at each step exactly, this model does that essentially on average. Moreover, the BFW model shows that the threshold of a giant component is $t = c^*n$ where c^* satisfies a certain transcendental equation and $c^* \in [0.9792, 0.9793]$. This result has been verified by theoretical methods [29] and simulations [30].

Recently, the BFW model is extended to the BFW (α) one and analyzed by W. Chen and R. M. D'Souza [30] by modifying the function $g(k)$ to $\alpha + 1/\sqrt{2k}$. It is shown that multiple giant components appear in a discontinuous percolation transition. Furthermore, with the value of α decreasing, the threshold will delay and the phase transition will be more explosive. In Ref. [32], the results of the BFW model on random graphs are expanded to lattices of different dimensions. In the following sections, we will discuss the reason and properties of these phenomena and provide theoretical analysis.

For the theoretical analysis on the BFW (α) model, the *BFW* (α) *algorithm* is shown as follows:

algorithm BFW (α)
1 **begin**
2 $A = \emptyset$;
3 $k = 2$;
4 $t = u = 1$;
5 e `is a randomly sampled edge;`
6 **while**($t < 2n$)
7 **begin**
8 l= `Maximal size of component in` $A \bigcup \{e\}$;
9 **if**($l \leq k$)
10 $A = A \bigcup \{e\}$;
11 $t = t + 1$;
12 $u = u + 1$;
13 `sample an edge` e `randomly;`
14 **else if**($t/u < \alpha + 1/\sqrt{2k}$)
15 $k = k + 1$;
16 **else**

```
17              u = u + 1;
18              sample an edge e randomly;
19      end
20 end
```

To analyze the evolution of the BFW (α) model and its steady-states, we consider the following variables: k, t, u and n possess the same meaning as they have in the BFW (α) algorithm; m represents the number of components; C_i denotes the fraction of the ith largest component.

In the BFW (α) algorithm, there are three cases when an edge is sampled:

- *Case* I: the vertices of sampled edge are in the same component;
- *Case* II: they are in two components C_i and C_j and $C_i + C_j \leq k/n$;
- *Case* III: they are in two components C_i and C_j and $C_i + C_j > k/n$.

According to the BFW (α) algorithm, we sample a random edge at step u: in Case I, the edge is also accepted; in Case II, the edge is also accepted and two components C_i and C_j merge together; in Case III, we should consider the constraint condition $t/u < \alpha + 1/\sqrt{2k}$ (on the 14th line of the BFW (α) algorithm). This constraint condition is the kernel hard core of the BFW (α) model, which ensures components increase either evenly or dramatically.

Let's first introduce a function $f_\alpha(t, u, k)$, which denotes the maximal acceptable value of Δk at one step (Δk is the change of k). Due to the BFW (α) algorithm, if the rate of accepted edges t/u is smaller than α, any sampled edge should be accepted; else, k can only increase until the condition $t/u < \alpha + 1/\sqrt{2k}$ is invalid. Thus, the function $f_\alpha(t, u, k)$ is shown as follows:

$$f_\alpha(t, u, k) = \begin{cases} \min\left\{x \in \mathbb{N}^+ \,\middle|\, \dfrac{t}{u} \geq \alpha + \dfrac{1}{\sqrt{2(k+x)}}\right\}, & \text{if } \dfrac{t}{u} > \alpha \\ n, & \text{if } \dfrac{t}{u} \leq \alpha. \end{cases} \tag{1}$$

According to the definition of f_α, when a random edge is sampled between two components C_i and C_j, if and only if $f_\alpha \geq n(C_i + C_j) - k$, we can accept the edge ($t \leftarrow t + 1$) and the components C_i and C_j merge together ($m \leftarrow m - 1$). Moreover, k can change by no more than $n(C_i + C_j) - k$ and $f_\alpha(t, u, k)$, so we have that in one step:

$$\Delta k = \min\left(n(C_i + C_j) - k, f_\alpha\right), \tag{2}$$

$$\Delta t = -\Delta m = \delta\left(n(C_i + C_j) - k, f_\alpha\right). \tag{3}$$

Here $\delta(x, y) = 1$ if $x \leq y$ and $\delta(x, y) = 0$ otherwise.

Let's define the function $P_{ij}(t, u, k)$ as the probability that the vertices of a sampled edge at step u are in C_i and C_j, $P_{ii}(t, u, k)$ as the probability that vertices are both in C_i. Then as u increases, the evolution equations of k, t and m are established as follows:

$$\frac{\mathrm{d}k}{\mathrm{d}u} = \sum_{C_i + C_j > k/n} \min\left(n(C_i + C_j) - k, f_\alpha\right) P_{ij}(t, u, k), \tag{4}$$

$$\frac{\mathrm{d}m}{\mathrm{d}u} = -P_2(t, u, k) - \sum_{C_i + C_j > k/n} \delta\left(n(C_i + C_j) - k, f_\alpha\right) P_{ij}(t, u, k), \tag{5}$$

$$\frac{\mathrm{d}t}{\mathrm{d}u} = P_1(t, u, k) + P_2(t, u, k) + \sum_{C_i + C_j > k/n} \delta(n(C_i + C_j) - k, f_\alpha) P_{ij}(t, u, k). \tag{6}$$

Here the function $P_1(t, u, k)$ is defined as the probability that the vertices of a randomly sampled edge at step u are in the same component (Case I); similarly, the function $P_2(t, u, k)$ is defined as the probability that they are in two components with the sum smaller than k (Case II). Therefore, we can simply obtain:

$$P_1(t, u, k) = \sum_{i=1}^{m} P_{ii}(t, u, k), \tag{7}$$

$$P_2(t, u, k) = \sum_{C_i + C_j \leq k/n} P_{ij}(t, u, k). \tag{8}$$

For Eq. (4), k is the upper bound of the size of the largest component and never changes in Cases I and II; only in Case III can k change by no more than $n(C_i + C_j) - k$ and $f_\alpha(t, u, k)$, i.e., $\Delta k = \min\left(n(C_i + C_j) - k, f_\alpha(t, u, k)\right)$. For Eq. (5), $\Delta m = 0$ in Case I and -1 in Case II respectively; in Case III, the number of components will decrease by 1 if and only if $f_\alpha \geq n(C_i + C_j) - k$, i.e., $\Delta m = -\delta\left(n(C_i + C_j) - k, f_\alpha\right)$. For Eq. (6), the sampled edge must be accepted in Cases I and II, so $\Delta t = 1$; similar to the m of Eq. (5) in Case III, an edge can be accepted when $f_\alpha \geq n(C_i + C_j) - k$ and $\Delta t = \delta\left(n(C_i + C_j) - k, f_\alpha\right)$.

3. Dynamical behaviors of BFW (α) model on random graph

On random graphs, the total number of edge is $O(n^2)$, but we only accept $t \sim 2n$ edges. So the probability of sampling an existing edge can be ignored when the size n is large enough. Function $P_{ii}(t, u, k) = C_i^2$ and $P_{ij}(t, u, k) = 2C_iC_j$, thus Eqs. (7) and (8) can be revised as follows:

$$P_1(t, u, k) = \sum_{i=1}^{m} C_i^2,$$
$$P_2(t, u, k) = 2 \sum_{C_i+C_j \le k/n} C_iC_j.$$

Combining with Eqs. (4)–(6), more information about the BFW (α) model can be obtained. We next provide a theoretical analysis about properties and behaviors of this model.

3.1. Steady-state conditions of evolution of the BFW (α) model

Although Eqs. (4)–(6) are unsolvable, some interesting properties and results can still be deduced from these equations, especially the steady-state conditions.

Taking the right side of Eqs. (4) and (5) as 0, we can obtain $P_2(t, u, k) = 0, \min\left(n(C_i + C_j) - k, f_\alpha\right) = 0$ and $\delta\left(n(C_i + C_j) - k, f_\alpha\right) = 0$. Furthermore, for two components with sum smaller than k, they must merge together, but the merging operation is forbidden after the system stabilizes, so any two giant components stay with $n(C_i + C_j) - k > 0$ after stabilizing, then the steady-state conditions can be simplified to be:

$$\begin{cases} f_\alpha(t, u, k) = 0 \\ P_2(t, u, k) = 0. \end{cases} \tag{9}$$

According to the definition, $f_\alpha(t, u, k) = 0$ if and only if $t/u > \alpha + 1/\sqrt{2k}$, so we just need to prove $t/u > \alpha + 1/\sqrt{2k}$ and $P_1(t, u, k) > \alpha$ are equivalent.

For $P_1(t, u', k) > \alpha$ with some u', we can prove that $t/u > \alpha + 1/\sqrt{2k}$ for any $u > u'$. Doing calculations on both sides of Eq. (6) from an initial state (t_0, u_0) to a current state (t_1, u_1), we have:

$$t_1 - t_0 = \int_{u_0}^{u_1} P_1 \, \mathrm{d}u + \int_{u_0}^{u_1} 2 \sum_{C_i+C_j>k/n} \delta(n(C_i + C_j) - k, f_\alpha) C_iC_j \, \mathrm{d}u$$
$$> \int_{u_0}^{u_1} P_1 \, \mathrm{d}u.$$

No matter how large u is, we can always find some $u_0 > u$ with $t_0/u_0 > \alpha$ because the BFW (α) model ensures the fraction of accepted edges is never smaller than α for ever. Suppose t/u is always smaller than α, by the rule of the BFW (α) model, the sampled edge must be accepted and t, u increase accordingly in each step, which will lead to the increase of the value of t/u and finally make $t/u > \alpha$.

For P_1, only when a sampled edge linking C_i and C_j is accepted, the part of $C_i^2 + C_j^2$ changes to $(C_i + C_j)^2$, which will make the value of $P_1(t, u, k)$ increase; otherwise, $P_1(t, u, k)$ will never change. So once $P_1(t, u, k) > \alpha$ for some u, it will be kept for ever.

In summary, once $P_1(t, u', k) > \alpha$ for some u', choosing $u_0 > u'$ with $t_0/u_0 > \alpha$, we obtain:

$$t_1 > t_0 + \alpha \int_{u_0}^{u_1} \mathrm{d}u > \alpha u_1.$$

Notice that the formula above is correct for any $u_1 > u_0$. After the giant components come up, we have:

$$k \sim nC_{\max} \sim O(n).$$

So $1/\sqrt{2k} \sim o(1)$ and it can be ignored when n is large enough. Therefore, when $P_1(t, u_1, k) > \alpha$ for any $u_1 > u'$, we obtain $t_1/u_1 > \alpha + 1/\sqrt{2k}$.

On the other hand, if $f_\alpha(t, u, k) = 0$ keeps for any $u > u'$, Eq. (6) turns out to be:

$$\frac{\mathrm{d}t}{\mathrm{d}u} = P_1(t, u, k).$$

In order to ensure $t/u > \alpha + o(1)(\forall u > u')$, we need the slope $P_1(t, u, k) > \alpha$. □

Finally, we can obtain the steady-state conditions for any $u > u'$:

$$\begin{cases} P_1(t, u, k) > \alpha \\ P_2(t, u, k) = 0. \end{cases} \tag{10}$$

In Fig. 1, simulations have verified this conclusion. For different values of α, the values of t/u and k/n change until $P_1(t, u, k) = \sum_{i=1}^{n} C_i^2 > \alpha$, which means the BFW ($\alpha$) system evolves until Eq. (10) takes effect.

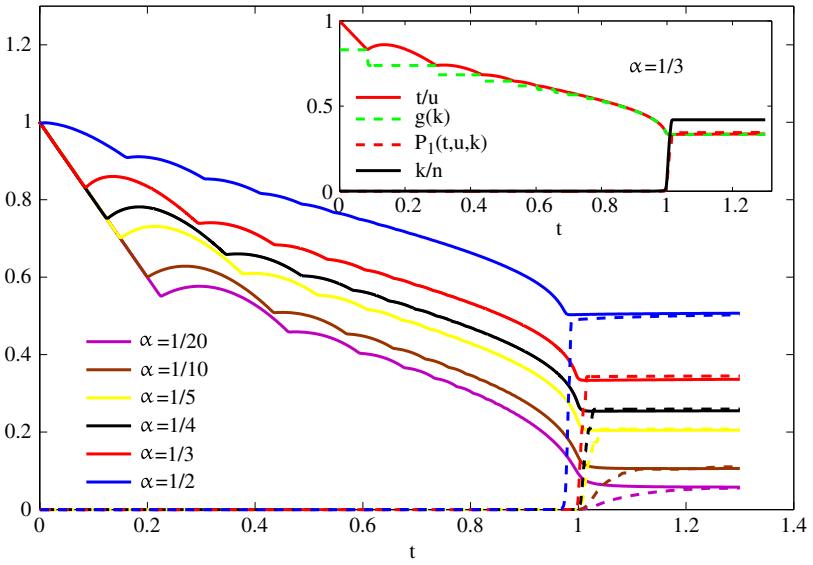

Fig. 1. Simulation of BFW (α) model by 100 random instances with $N = 10^6$ nodes. The solid lines denote the fraction of accepted edges for different values of α, which can be calculated by t/u in the algorithm; the dashed lines denote $P_1(t, u, k) = \sum_{i=1}^{100} C_i^2$. The above subgraph shows the dynamical evolution of variables k/n, t/u and $P_1(t, u, k)$ with $\alpha = 1/3$. By the results, when $P_1(t, u, k) > \alpha$, t/u stays greater than α and k keeps still.

3.2. Merging mechanism on the multiple giant components of BFW (α) model

Since in Cases I and II, sampled edges are always accepted, we just need to explicitly consider Case III. To obtain the maximal accepted change of k, i.e. f_α, we set $t/u = \alpha + 1/\sqrt{2k}$ and differentiate u on both sides by k [30]:

$$\frac{\mathrm{d}u}{\mathrm{d}k} = \frac{1}{2\sqrt{2}\left(\alpha + \sqrt{1/2k}\right)^2}\frac{t}{k^{3/2}}. \tag{11}$$

Before the giant component appears, we consider that $t \sim O(n)$, $k \sim nC_i \sim o(n)$. With $\mathrm{d}u = 1$ and Eq. (11), we obtain $f_\alpha \sim \mathrm{d}k \sim O(k^{\frac{3}{2}}/n)$. Let $\mathcal{S}$ denote the component set $\{C_i \mid k/2 < C_i n < k\}$. If the sampled edge links components C_i and C_j, where $C_i, C_j \in \mathcal{S}$, then $n(C_i + C_j) - k \sim O(k) \gg O(k^{\frac{3}{2}}/n)$. That leads to $\delta\left(n(C_i + C_j) - k, f_\alpha\right) = 0$, which means this edge is rejected. So the edge linking two components of $\mathcal{S}$ must be rejected and only the edge linking to at least one component of $\complement\mathcal{S}$ ($\complement\mathcal{S}$ is the complementary set of $\mathcal{S}$) can be accepted. For the process to be performed successively, either a new member in $\mathcal{S}$ comes up or the scale of an original one in $\mathcal{S}$ becomes more close to k. That is the key for coexisting multiple giant components, and they are expected to grow simultaneously before a critical point (Fig. 2).

Similarly, after the giant components appear, $k \sim nC_i \sim O(n)$, $\forall C_i \in \mathcal{S}$, so we have:

$$f_\alpha(t, u, k) \sim O(n^{1/2}) \ll n(C_i + C_j) - k. \tag{12}$$

Then we still have $\delta\left(n(C_i + C_j) - k, f_\alpha\right) = 0$ and the members of $\complement\mathcal{S}$ keep merging into $\mathcal{S}$ until $P_2 = 0$. According to the steady-state conditions Eq. (10), if C_i satisfies $P_1 > \alpha$, the system will stabilize; else, $P_1(t, u, k)$, which is the probability that the vertices of the sampled edge are in the same component, is smaller than α. As it is proved above, if $P_1 < \alpha$, we can always have some u with $t/u < \alpha + 1/\sqrt{2k}$, which makes k keep increasing (the 14th and 15th lines of the algorithm) until two components merge together.

Furthermore, only two minimal components (marked as $C_1^{\min}$, $C_2^{\min}$) can merge together. We define P as the probability of any two other components (marked as C_i, C_j) merging together before the two minimal ones, then

$$P \leqslant \left(1 - 2C_1^{\min}C_2^{\min}\right)^{n(C_i+C_j-C_1^{\min}-C_2^{\min})/\overline{f_\alpha(t,u,k)}}. \tag{13}$$

For one step, $\Delta k = \min\left(n(C_i + C_j) - k, f_\alpha\right) = f_\alpha$. Let's take $\overline{f_\alpha(t, u, k)}$ as the average increase of k for one step. Based on Eq. (12), $\overline{f_\alpha(t, u, k)} \sim O(n^{1/2})$. When k increases to be larger than $n(C_1^{\min} + C_2^{\min})$ but smaller than $n(C_i + C_j)$, only one edge linking $C_1^{\min}$ and $C_2^{\min}$ is sampled to make them merge together. So in order to ensure that $C_1^{\min}$ and $C_2^{\min}$ can't merge together before C_i and C_j, we need k to increase by $n(C_i + C_j - C_1^{\min} - C_2^{\min})$ without any components merging, which means $n(C_i + C_j - C_1^{\min} - C_2^{\min})/\overline{f_\alpha(t, u, k)}$ edges not linking $C_1^{\min}$ and $C_2^{\min}$ should be added. So the probability P satisfies Eq. (13).

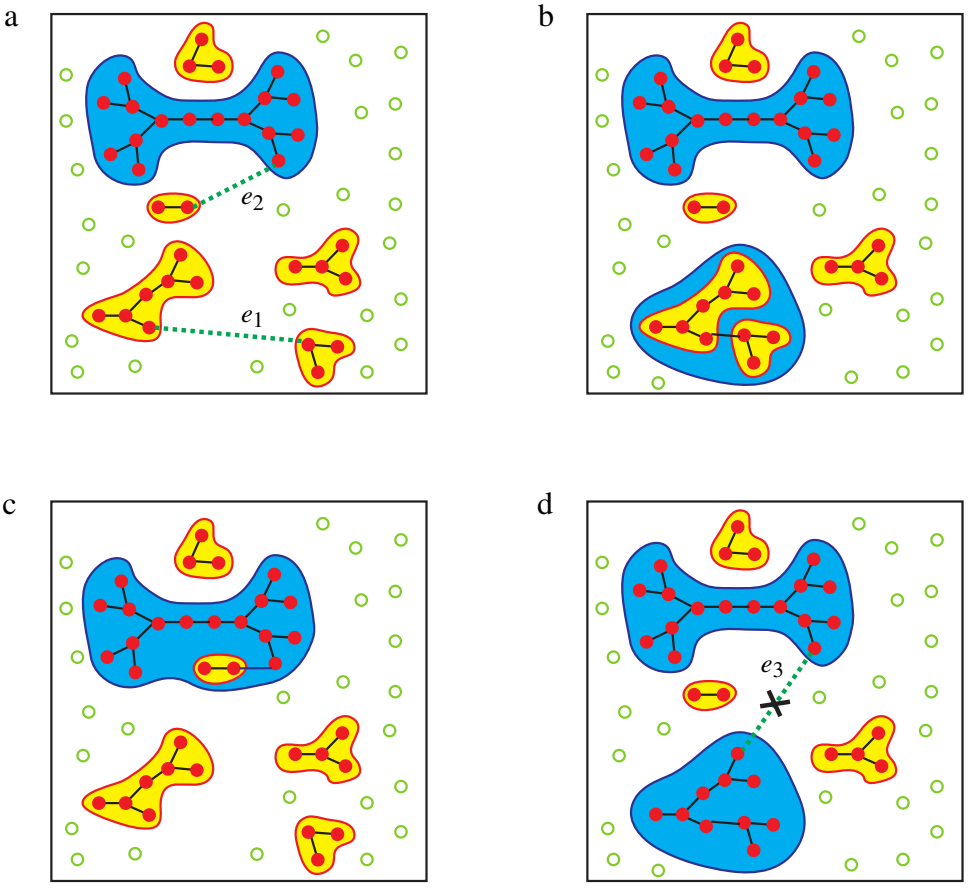

Fig. 2. An example for the evolution of BFW (α) model. System consists of $n = 60$ nodes. Subgraph (a) provides the initial graph at some step u, in which $k = 16$ and $t = 29$. At this step, two random edges (e_1, e_2) are picked yet only one is added to the graph based on the selection rule of BFW (α) model, whereas the other is discarded. The blue (yellow) components are (not) in the set $\mathcal{S}$. The green circles denote the isolated nodes. Subgraph (b) is the situation of adding edge e_1, two components of set $\mathbb{C}\mathcal{S}$ merge into the one of set $\mathcal{S}$. Subgraph (c) is the situation of adding edge e_2, a component of $\mathbb{C}\mathcal{S}$ merges into set $\mathcal{S}$, forming a new member of set $\mathcal{S}$. In subgraph (d), after the situation of subgraph (b) happens, there are more than one members in set $\mathcal{S}$. All the sampled edges linking two components in set $\mathcal{S}$ will be rejected, such as edge e_3. (For interpretation of the references to colour in this figure legend, the reader is referred to the web version of this article.)

As the system size $n \to \infty$, the number of needed edges $n(C_i + C_j - C_1^{\min} - C_2^{\min})/\overline{f_\alpha(t, u, k)} \to O(n^{1/2}) \to \infty$, causes $P \to 0$, which means two minimal components can merge before any two other components. This phenomenon can also be verified by simulation of the BFW (α) model (Fig. 3).

According to the discussion of the impact of a single edge added to the graph in Ref. [36], three distinct mechanisms which may contribute to increasing the size of the maximal component are identified:

(i) *Direct growth*: a smaller one merges into the maximal component;
(ii) *Overtaking*: two smaller components merge together to create a new maximal one;
(iii) *Doubling*: two components both of maximal size merge together to double the size of the original one.

With the analysis of the evolution mechanism of the BFW model above, we can recognize which kind of growth it is in the BFW model. Before the giant components appear, only the edge linking at least one component of $\mathbb{C}\mathcal{S}$ can be accepted, and it means the maximal component C_1 may increase by overtaking [36] or by merging with a tiny component of $\mathbb{C}\mathcal{S}$, which is essentially an isolated node [31]. After the giant components emerge but the system is not stabilized, the members of $\mathbb{C}\mathcal{S}$ will keep merging into $\mathcal{S}$ until $P_2 = 0$, the maximal component C_1 may increase over almost all by overtaking. Since the BFW model restricts the increase of the maximal component, the merging between a member of $\mathbb{C}\mathcal{S}$ and a non-maximal member of $\mathcal{S}$ can minimize the increase, which makes the maximal component grow by overtaking. Finally, we prove that only two minimal components in $\mathcal{S}$ can merge together, i.e. the maximal component C_1 may increase only by overtaking (Fig. 3).

3.3. Quantitative properties of the giant components of BFW (α) model

Since we have analyzed the BFW (α) model with fixed α in detail, in this section, we are going to calculate the number and size of giant components with arbitrary α in theory. Taking $C_i^m(\alpha)$ as the ith largest giant component of the steady-

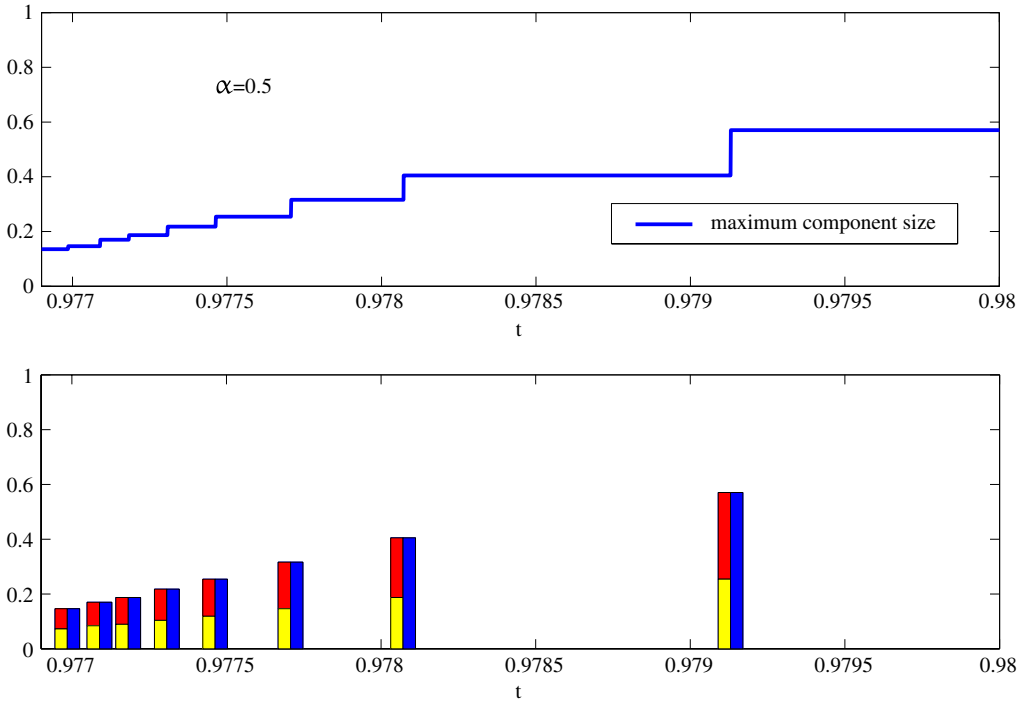

Fig. 3. Top: the maximal component's size in critical interval of the BFW (α) process; the horizontal axis t reflects a "jump point" at which the maximal component increases dramatically. Bottom: the yellow and red rectangles represent the first and second minimal components before "jump point", and the blue ones represent the maximal component after "jump point". At the "jump point", the two minimal components merge into the maximal one. All the other components in $\mathcal{S}$ stay unchanged at "jump point". That shows the growth of the maximal component is *overtaking* [36]. (For interpretation of the references to colour in this figure legend, the reader is referred to the web version of this article.)

state with m giant components (*m-steady-state*) to replace C_i above, we will find some common properties of $C_i^m(\alpha)$ when α belongs to some intervals.

3.3.1. Steady states with different evolution parameter α

In the BFW (α) model, the parameter α plays a key role in the problems of when the system can stabilize and which state the system can stabilize in. Defining $(\alpha_{m+1}, \alpha_m]$ as the m-steady-state interval in which there exist m giant components, $m = 1, 2, 3, \ldots$, for any α with $\alpha_{m+1} > \alpha \geqslant \alpha_m$, the values of $C_i^m(\alpha)$ are all the same when the system stabilizes (Fig. 4), so we take C_i^m instead of $C_i^m(\alpha)$ briefly for all $\alpha \in (\alpha_{m+1}, \alpha_m]$. Thus, the members in the set $\mathcal{S}$ evolve similarly with different phases in different intervals of α.

Moreover, if system *BFW* (α) with $\alpha \in (\alpha_{m+1}, \alpha_m]$ has $m+1$ components $C_i^{m+1}(\alpha)$ in $\mathcal{S}$, there must be $P_1(t, u, k) < \alpha$, which leads to its collapse and a steady phase of *m-steady-state*. As mentioned above, Eq. (13) ensures that only the two minimal components can merge before the system stabilizes and they merge to the largest one in *m-steady-state* (Fig. 3). So the C_i^m and C_i^{m+1} must satisfy:

$$C_{i+1}^m = C_i^{m+1}, \quad \forall i = 1, 2, \ldots, m-1. \tag{14}$$

In addition, when two components merge together, $P_1(t, u, k)$ will "jump" by $(C_{m+1}^{m+1} + C_m^{m+1})^2 - (C_{m+1}^{m+1})^2 - (C_m^{m+1})^2 = 2C_m^{m+1}C_{m+1}^{m+1}$. Notice that in *m-steady-state*, $P_1(t, u, k)$ stays unchanged and is larger than $\alpha \in (\alpha_{m+1}, \alpha_m]$, so $P_1(t, u, k)$ must be the upper bound of α in *m-steady-state*:

$$\sum_{i=1}^{m} (C_i^m)^2 = \alpha_m. \tag{15}$$

Suppose all components' sizes in $\mathcal{S}$ are very close and $\sum_{i=1}^{m} C_i \simeq 1$, we have the theoretical expression of α_m:

$$\alpha_m = \sum_{i=1}^{m} (C_i^m)^2 = \sum_{i=1}^{m} \frac{1}{m^2} = \frac{1}{m}. \tag{16}$$

As the value of α goes smaller, the assumption is closer to the truth by numerical results (Fig. 5). Considering the evolution process of the BFW model discussed above, the members of $\complement\mathcal{S}$ keep merging into $\mathcal{S}$ without increasing the value of k too

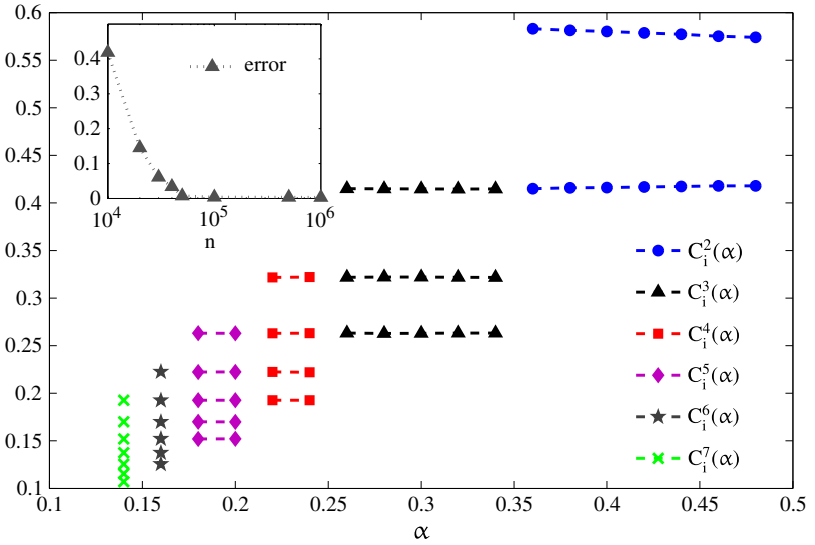

Fig. 4. Size of giant components in set $\mathcal{S}$ with different α. Circles, triangles, squares, diamonds, stars and crosses denote the fraction of giant components in steady-state of $m = 2, 3, \ldots, 7$ respectively. The results are obtained by 100 random instances with 10^6 nodes. The above subgraph denotes the scaling of the error of all $|C_i^{m+1} - C_{i+1}^m|$ for every $m = 2, 3, \ldots, 7$ and $i \in [1, m-1]$. Here the C_i^m is average size of ith largest component in *m-steady-state* by simulations.

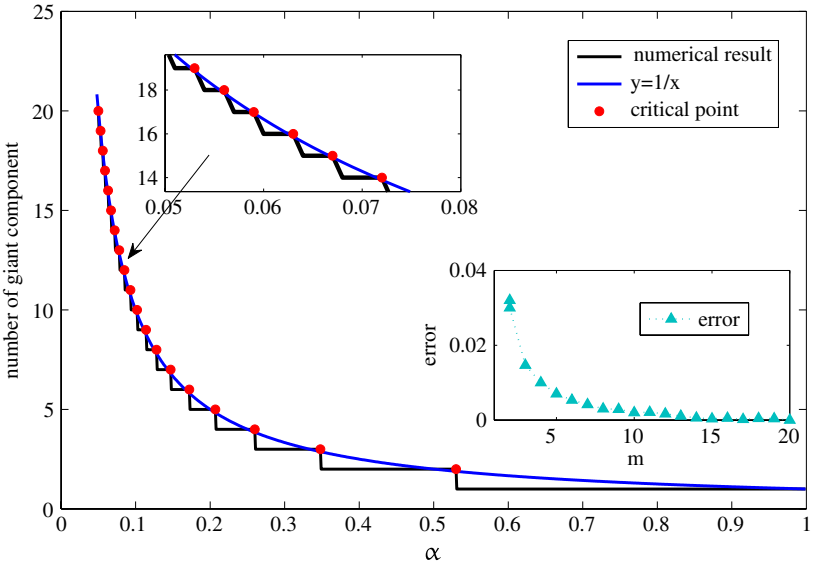

Fig. 5. Critical points of phase transition of stable giant components' number for $\alpha \in [0.05, 1]$. The red solid circles and black lines represent numerical results of 100 random instances with 10^6 nodes. The blue lines denote theoretical results. The solid triangles in the lower subgraph denote the error between numerical and theoretical results. (For interpretation of the references to colour in this figure legend, the reader is referred to the web version of this article.)

much; this is the kernel point to ensure that the multiple giant components emerge and the percolation is discontinuous. The members of the set $\mathcal{S}$ will grow evenly and slowly and the sizes of them are very close. With the smaller value of α, we prove that the system will stabilize in the steady-state of more giant components, the growth of components in the set $\mathcal{S}$ will be more uniform. As increasing the value of α, the system will evolve to the next steady-state of fewer giant components, the errors of the previous state will accumulate and finally become a large deviation between theoretical results and simulations.

3.3.2. Number and sizes of multiple giant components

Firstly, we can take the whole set $\mathcal{S}$ as a component and assume it grows similarly as the giant component on Erdös–Rényi random graphs, in which the number of added edges is expected to be the sampled edge number u. As rejected edges are almost between two components of $\mathcal{S}$, the size of the whole set $\mathcal{S}$ is almost unchanged if we take these rejected edges on. According to the method of generating function [37], the fraction x of giant component satisfies the equation $1 - x = e^{-2xu/n}$,

Table 1
The fraction of components, P_1 and fraction of the whole set $\mathcal{S}$ with $\alpha = 1/2, 1/3, 1/4, 1/5$. The results are obtained by 100 random instances with 10^6 nodes. The numbers in brackets are theoretical results, which are obtained by Eqs. (14)–(17).

	$\alpha = 1/2$	$\alpha = 1/3$	$\alpha = 1/4$	$\alpha = 1/5$
C_1	0.5736	0.4142	0.3220	0.2631
C_2	0.4144	0.3217	0.2629	0.2223
C_3		0.2633	0.2223	0.1926
C_4			0.1928	0.1699
C_5				0.1519
$\sum C_i^2$	0.5007 (0.5000)	0.3444 (0.3333)	0.2594 (0.2500)	0.2077 (0.2000)
x_m	0.9880 (0.9802)	0.9992 (0.9975)	0.9999 (0.9997)	0.9998 (0.9999)

where u represents the number of added edges. At the critical point, the threshold $t_c \simeq 1$ and $t_c/u \simeq \alpha$ when u is large enough (Fig. 1). With Eq. (15), we obtain the general equations of the fraction of giant components C_i^m for any integer m:

$$\begin{cases} \sum_{i=1}^{m} (C_i^m)^2 = \alpha_m \\ \sum_{i=1}^{m} C_i^m = x_m \\ 1 - x_m = \mathrm{e}^{-2x_m/\alpha}. \end{cases} \tag{17}$$

Here x_m denotes the fraction of the whole set $\mathcal{S}$ which has m giant components. Notice for case $m = 2$, Eq. (17) can be solved uniquely (due to the error of α_m in Fig. 5, the accurate result $\alpha_m = 0.52$ is adopted), then with the results and Eq. (14), we can obtain all the sizes of multiple giant components. The contrast between theory and simulation is shown as follows (see Table 1).

In summary, the parameter α determines when the system can stabilize and which state the system can stabilize in. In the evolution process of the BFW (α) model, α can only take effect on the time to increase k. As to how much k increases, α doesn't work. With this special evolution rule of the BFW (α) model, the connection between two adjacent steady-states is found and sizes of giant components are obtained. As the value of α decreases, theoretical results can be much better and it is verified by simulations.

4. Dynamical behaviors of BFW (α) model on finite-dimensional lattice

Different from random graphs, the total number of edges on a finite-dimensional lattice is $E \sim O(dn)$, where d is the dimension of the lattice and n is the number of vertices. If t edges have been added to the lattice at step u, the probability of sampling a random edge at the next step is $\theta(t) = 1 - t/E$. In mean-field theory, no matter what the structures of the components are and only considering which component the vertices of the random sampled edge belong to, we have functions $P_{ij}(t, u, k) = 2\theta(t)C_iC_j$ and $P_{ii}(t, u, k) = \theta(t)C_i^2$. So on a d-dimensional lattice, the right side of Eqs. (4)–(6) should be revised by multiplying by the factor $\theta(t)$ and the exact form will be:

$$\frac{\mathrm{d}k}{\mathrm{d}u} = 2\theta(t) \sum_{C_i+C_j>k/n} \min\left(n(C_i + C_j) - k, f_\alpha\right) C_iC_j, \tag{18}$$

$$\frac{\mathrm{d}m}{\mathrm{d}u} = -\theta(t)P_2(t, u, k) - 2\theta(t) \sum_{C_i+C_j>k/n} \delta\left(n(C_i + C_j) - k, f_\alpha\right) C_iC_j, \tag{19}$$

$$\frac{\mathrm{d}t}{\mathrm{d}u} = \theta(t)(P_1(t, u, k) + P_2(t, u, k)) + 2\theta(t) \sum_{C_i+C_j>k/n} \delta(n(C_i + C_j) - k, f_\alpha)C_iC_j. \tag{20}$$

Notice that with t increasing, $\theta(t)$ decreases to 0. Thus, the steady-state conditions on random graphs (Eq. (10)) are invalid because $P_1(t, u, k) > \alpha$ doesn't ensure $t/u > \alpha + 1/\sqrt{2k}$ any more. Only when $\theta(t) = 0$, i.e. $t = E$, can the system stabilize. Actually the steady-state on finite-dimensional lattices is a complete graph with one component, which is different from the result of multiple giant components on random graphs. However, with t increasing, some *metastable-states* appear and can stabilize for a period of time, in which multiple giant components coexist. Then, we will introduce the metastable-state phenomenon on finite-dimensional lattices, which is very similar to random graphs.

For Eqs. (18)–(20), as in what we do on random graphs, suppose $P_1(t, u, k) > \alpha$ and $P_2(t, u, k) = 0$ and we have:

$$\frac{\mathrm{d}t}{\mathrm{d}u} = \theta(t)P_1(t, u, k). \tag{21}$$

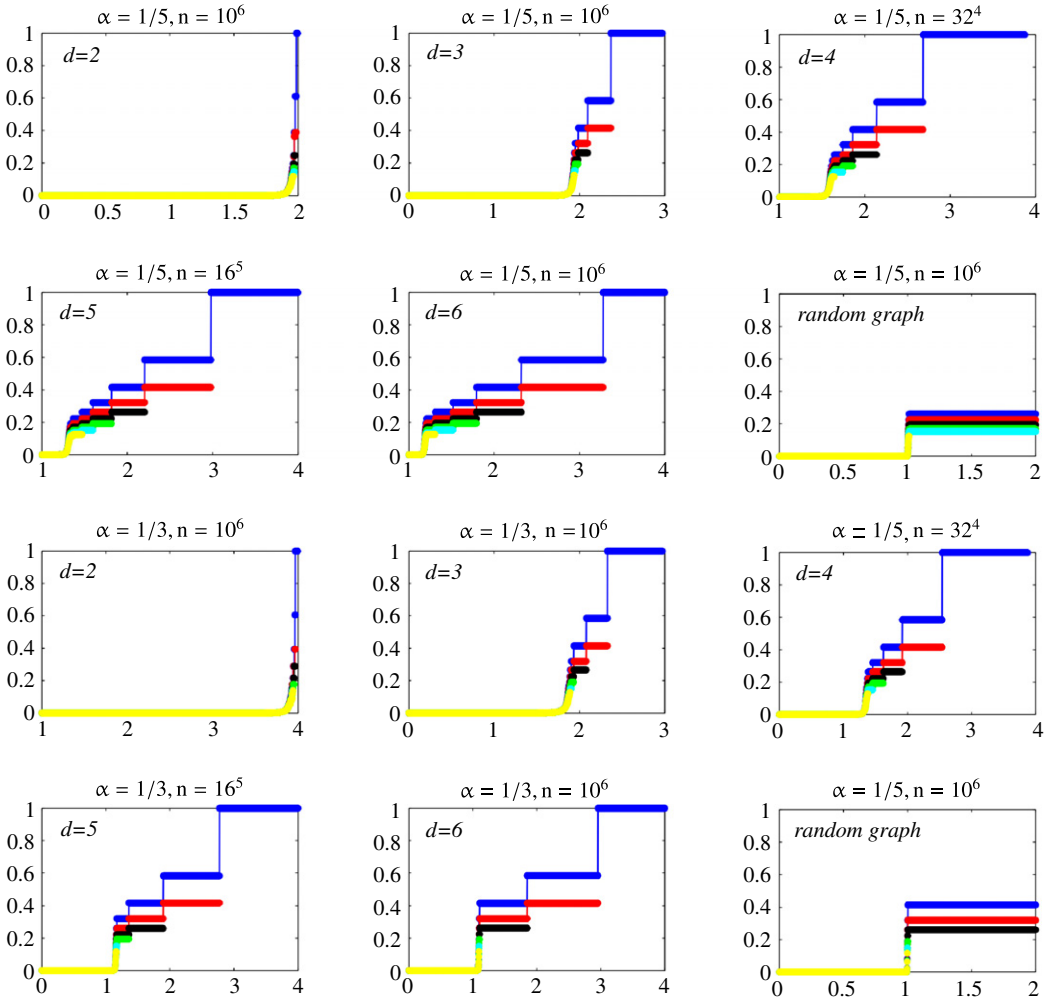

Fig. 6. The process of BFW (α) model on different dimensional lattices of $d = 2, 3, 4, 5, 6$ and random graphs. Here $\alpha = 1/5$ and $1/3$. The system size n is almost 10^6 (for $d = 4, 5$ it is 32^4 and 16^5). The horizontal and longitudinal axes denote t/n and fractions of vertices in components respectively. Different components are distinguished by the colors (from large to small: blue, red, black, green and cyan). We can see several "metastable-states" with multiple giant components on finite-dimensional lattices during the process, which correspond to the steady-states on random graphs accurately. (For interpretation of the references to colour in this figure legend, the reader is referred to the web version of this article.)

As proved on random graphs, the steady-state condition on finite-dimensional lattices should be $\theta(t)P_1(t, u, k) > \alpha$, for all $t > t_0$. But $P_1(t, u, k) \leq 1$ and with t increasing, the factor $\theta(t)$ keeps decreasing to 0. So the slope of t versus u will finally become smaller than α, which makes $t/u < \alpha$ and $f_\alpha > 0$. So condition $\theta(t)P_1(t, u, k) > \alpha$ is invalid on finite-dimensional lattices. Only when t increases up to E, i.e. $\theta(t) = 0$, will the system stabilize to a complete graph, which has only one component (Fig. 6).

The phenomenon on random graphs is different from that on finite-dimensional lattices (Fig. 6). On random graphs, $O(n^2)$ edges can be sampled and added. According to the rule of the BFW (α) model, the edges linking two vertices of the same component are preferred to be accepted. That means $O((C_i n)^2)$ edges in component C_i can be added without any restraint. In contrast, for the stable system in the thermodynamic limit, there are $O(dn)$ edges on finite-dimensional lattices, which is linear to n. So the system can stabilize only when the edges are all added to graphs.

Furthermore, there are also some "*m-metastable-states*" (stabilizing with m giant components for a period of time) during the evolution process on finite-dimensional lattices, which are similar to the *m-steady-states* on random graphs. Every system on finite-dimensional lattices must experience all the *m-metastable-states* ($m \in [1/\alpha, 1]$) and reach the steady-state. This phenomenon is much similar to what it does on random graphs. Based on the evolution Eqs. (18)–(20), all the analysis and conclusions obtained on random graphs are applicable to finite-dimensional lattices. They have the same dynamical behaviors and merging mechanism. Let's take $\alpha' = \alpha/\theta(t)$ as the substantial parameter of the system, then, by Eq. (21) the steady-state condition on finite-dimensional lattices will be:

$$P_1(t, u, k) > \alpha'.$$

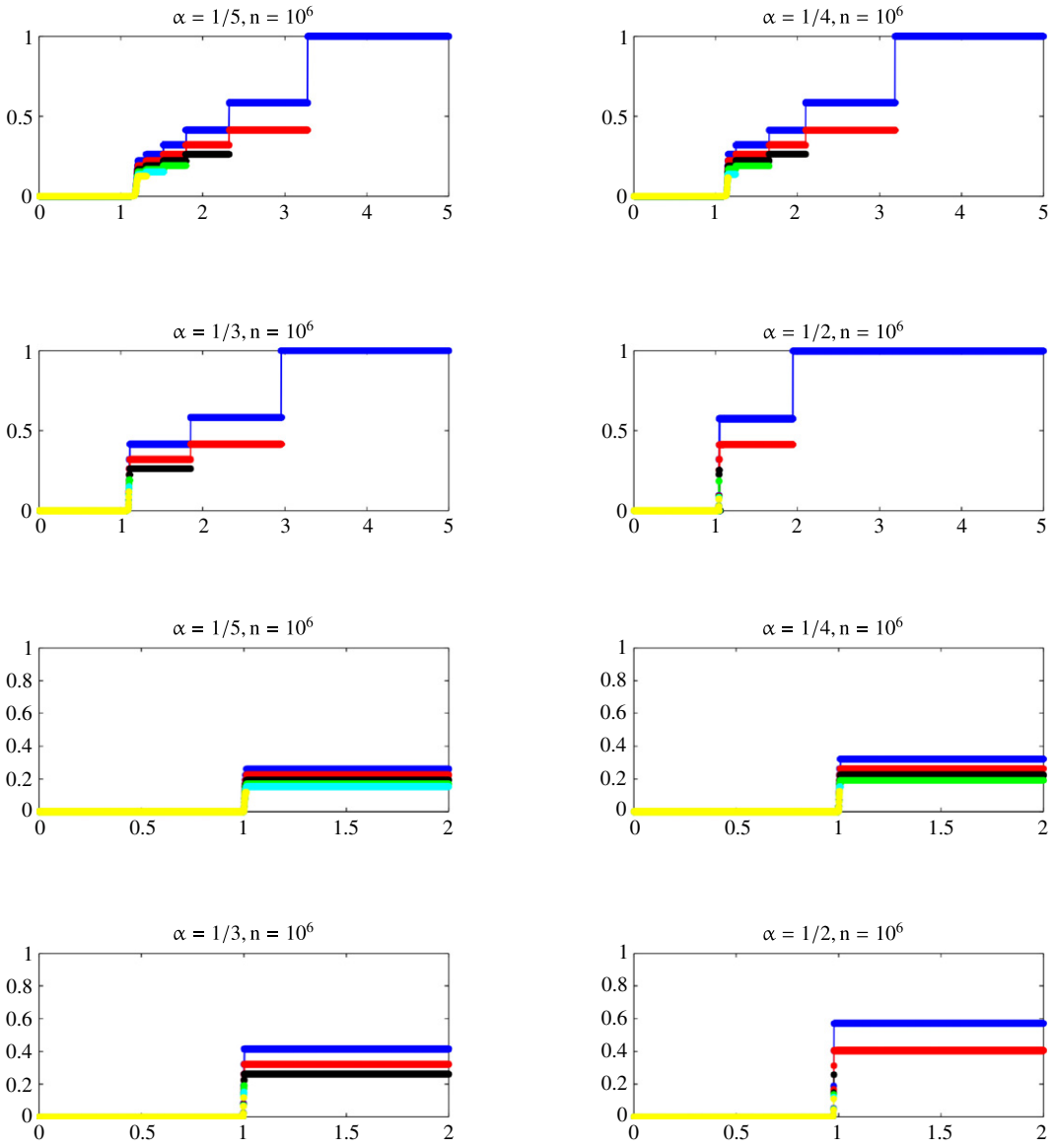

Fig. 7. The process of BFW (α) model on 6-dimensional lattice (top) and random graph (bottom) with different values of $\alpha = 1/5, 1/4, 1/3, 1/2$. Colors and axes are the same as in Fig. 6. After the critical point, multiple giant components appear and coexist for a short time. On growing by "*overtaking*", these components finally merge together. Correspondingly, you can see the relationship and difference between finite-dimensional lattice and random graph with the same parameter α.

As t increases, the parameter α' will change from α to 1 (though α' can be infinity, the upper bound of 1 is large enough for our analysis). As in what we analyzed on random graphs, the system on a lattice will stabilize on some metastable-state until the change of parameter α' causing $P_1(t, u, k) < \alpha'$. At this time, the system will evolve to the next metastable state, and keep doing this until reaching the steady-state. In every metastable-state, the slower the parameter α' changes, the longer the system will be steady. Moreover, the changing speed of α' depends on the factor $\theta(t) = 1 - t/O(dn)$, so with the same size n, the system will stay longer in every metastable-state on the lattice with larger dimensions (Fig. 6).

In Fig. 7, it shows the process on a 6-dimensional lattice and random graph with varying parameter α. We can see the phenomenon related to the change of α' clearly on the top four subgraphs. From the critical point, the metastable-state with multiple giant components appears. With t increasing, the system evolves to the next metastable-state with fewer components, which indicates the substantial parameter α' increasing. Finally, the system reaches the steady-state with one component, and now the parameter α' has increased larger than 1. On the bottom four subgraphs, these are the counterparts on random graphs. Compared to the lattices, it is clear that the system on random graphs stabilizes on the m-steady-state, which is just the m-metastable-states on lattices. The number and size of components between the m-steady-state and m-metastable-states are exactly the same for different values of α.

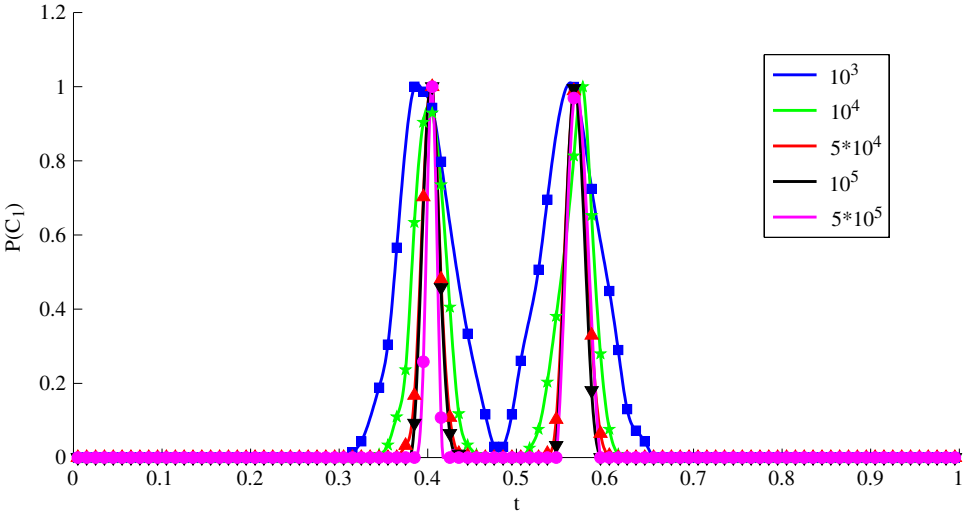

Fig. 8. Distribution of the parameter C_1 for different size n on random graph. They are shown at the effective critical point, which is defined such that both peaks have the same height. Normalization is such that their height is 1. The points are the results of simulation with 1000 independent realizations for different n. Curves are approximated by cubic splines to make them smooth.

5. The scaling properties and nonlocality of BFW (α) model

We establish the explosive properties of the BFW (α) model on both random and finite-dimensional lattices via theoretical methods and numerical simulation. Next, we analyze the scaling behavior on the BFW (α) model. For infinite size n, the size of maximal component $C_i n$ jumps at the critical point t_c if the transition is discontinuous, while if it varies continuously with a power law singularity $C_i n \sim (t - t_c)^{\beta}$ for a continuous transition [16]. Many models have been proved continuous based on the scaling behaviors [15,17]. As analyzed above, it is accurately described that the growth of the maximal component is by overtaking (Fig. 3) and only the two minimal components in set $\mathcal{S}$ can merge together (Eq. (13)). So the size of the maximal component must jump at the critical point, which means the transition of the BFW (α) model is discontinuous. In Fig. 8 is shown the distribution of C_1 at the critical point. With the size n increasing, the distance between two peaks increases and the distribution approaches a binomial distribution. Based on the evolution mechanism of the BFW (α) model, two minimal components in set $\mathcal{S}$ merge together causing the growth of maximal one by overtaking. So there are several "jumps" occurring before the system stabilizes; we just show the biggest "jump" in Fig. 8.

Meanwhile, according to the studies about locality and nonlocality on the other models [11,38], the BFW (α) model is typically nonlocal. We find that nonlocality of the BFW (α) model contributes very much to the *overtaking*, which finally causes the discontinuous phase transition. It is a strong restriction that the BFW (α) model uses the nonlocal information to control the size of the maximal component. On increasing the value of α, the restriction will decline, the frequency of growth by overtaking will also decrease, and it will be instead from *direct growth*. With removing the restriction, i.e. $\alpha = 1$, this model becomes the original ER model, which is a continuous transition.

Additionally, let $\Delta_n(\gamma, A)$ denote the number of edges required for C_1 to go from size $C_1 n \leq |n^{\gamma}|$ to $C_1 n \geq |An|$. We want to prove that $\lim_{n\to\infty} \Delta_n(\gamma, A)/n = 0$, which also means the transition is discontinuous [11]. See Fig. 9, at some step u, we always have $t/u = \alpha + 1/\sqrt{2k}$, and the slope of t versus u is $P_1(t, u, k)$. So the maximal number of accepted edges (marked X in Fig. 9) before C_1 grows can be obtained:

$$X = \frac{P_1}{(\alpha - P_1)\sqrt{2k}}. \tag{22}$$

Integrating Eq. (22) from $k = n^{\gamma}$ to $k = An$, we have:

$$\Delta_n(\gamma, A) = \int_{n^{\gamma}}^{An} \frac{P_1}{(\alpha - P_1)\sqrt{2k}}\, dk \leq B \int_{n^{\gamma}}^{An} \frac{1}{\sqrt{2k}}\, dk = B\sqrt{2k}\Big|_{k=n^{\gamma}}^{k=An}.$$

Here B denotes the upper bound of $P_1/(\alpha - P_1)$. P_1 is a monotonically nondecreasing function and $P_1 < \alpha$ before the system stabilizes, so the function $P_1/(\alpha - P_1)$ is bounded. The $\lim_{n\to\infty} \Delta_n(\gamma, A)/n = 0$ can be proved and the transition of the BFW (α) model is discontinuous. It can be verified by simulation in Fig. 10. Notice Eq. (22) above is applied on the random graph, and on lattices P_1 should be changed to $\theta(t)P_1$. The same operation can be expanded to lattices because the factor $\theta(t)$ is also bounded.

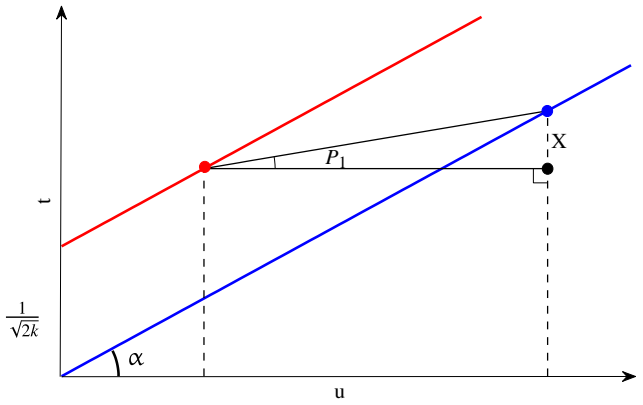

Fig. 9. The blue line represents $t/u = \alpha$ and the red line $t/u = \alpha + 1\sqrt{2k}$. Let's take the red solid circle as the beginning point at some step u and the direction of advance now is P_1. According to the rule of BFW (α) model, any sampled edge should be accepted when the point goes below the blue line $(t/u < \alpha)$, even though that would make C_1 grow dramatically. So the maximal number of accepted edges for growth of C_1 is marked as X, which is the distance between blue solid circle and black solid circle. (For interpretation of the references to colour in this figure legend, the reader is referred to the web version of this article.)

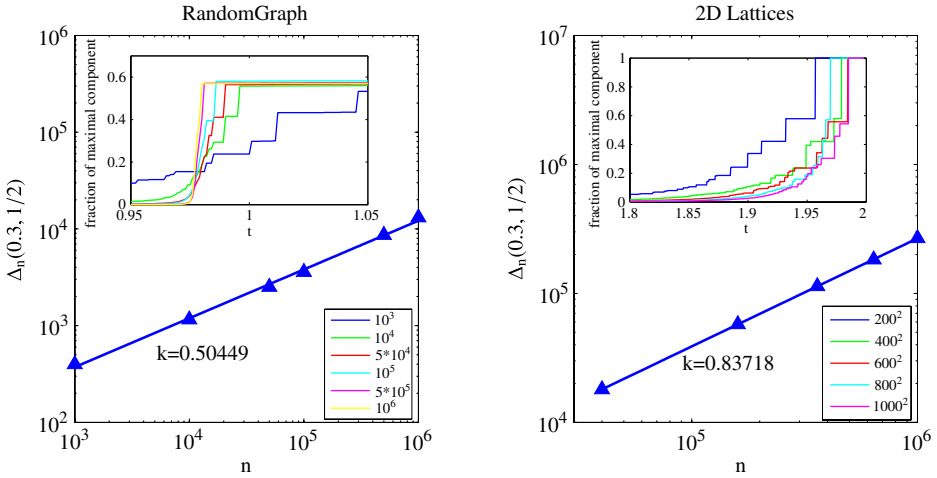

Fig. 10. $\Delta_n(0.3, \frac{1}{2})$ versus the size of the system on random graph and 2-dimensional lattice. The blue triangles represent the average number of added edges from $C_1 n \sim n^{0.3}$ to $C_1 n \sim \frac{1}{2} n$, which are obtained by averaging 1000 independent realizations for different n. The results yield the blue line and k is the slope. Inset: the fraction of maximal component versus edge density with varying n, the sizes of the system are distinguished by the colors on the bottom. (For interpretation of the references to colour in this figure legend, the reader is referred to the web version of this article.)

6. Conclusion and discussion

We detect the steady-state and evolution process of the BFW (α) model with both numerical and theoretical methods on random graphs and finite dimensional lattices. According to the rule of the BFW (α) model, the function f_α is defined to calculate the change of the stage k and number of giant components m. Furthermore, by establishing the mathematical expression of evolution equations on this model, a relationship between the parameter α and steady-state condition is proved. Meanwhile, with some hypothesis, the correspondence between the parameter α and the number of giant components in steady-state is obtained, that is when $\alpha \in (\frac{1}{m+1}, \frac{1}{m}]$, the BFW (α) model must stabilize with m giant components. Through the further analysis of the evolution process and the numerical results, the set $\mathcal{S}$ is defined to find the rule of two components merging before and after the threshold. Moreover, the sizes of giant components for different evolution strategies also have a close connection with each other and satisfy some constraint equations, which are derived from the evolution equations. The similar conclusion can be expanded to finite-dimensional lattices.

So far, on random graphs, we can calculate the number and sizes of giant components for different evolution strategies with theoretical methods, which fit very closely with the simulations, especially when the value of α is smaller than 0.25. As to finite-dimensional lattices, the steady-state must be a complete graph, but there are some metastable states during the evolution process, in which the number and sizes of multiple giant components are the same as those on related random graphs. Additionally, the analysis of the steady-state and evolution process is of great help to explain why the percolation of the BFW (α) model is discontinuous and how dramatic the transition is, which is almost supported before by simulations.

For example, before the giant component appears, we can obtain $\mathrm{d}k/\mathrm{d}t \sim O(k^{\frac{3}{2}}/n)$, although the $k \sim O(n^{\frac{2}{3}+\delta}) \sim o(n)$, for $0 < \delta < 1/3$, we still have $\mathrm{d}k/\mathrm{d}t \sim \infty$; here $k \sim C_{\max}$, so the result means percolation of the BFW (α) model is dramatically discontinuous. Finally, we find the nonlocality on the BFW (α) model decides the growing mechanism of the maximal component.

Besides, we just analyze this model on Erdös–Rényi random graphs and finite-dimensional lattices; as to other structures with any degree distribution, the theoretical framework in this paper also works, in which we only need to modify the related probabilities in the evolution equations. As to the nature of discontinuous transitions on other models and how to apply this method to real systems, future work must bridge the gap and establish a universal framework.

Acknowledgment

This work is supported by the Fundamental Research Funds for the Central Universities and National Natural Foundation of China No. 11201019.

References

[1] D. Stauffer, A. Aharony, Introduction to Percolation Theory, second ed., Taylor & Francis, London, 1994.
[2] M. Sahimi, Applications of Percolation Theory, Taylor & Francis, London, 1994.
[3] R. Pastor-Satorras, A. Vespignani, Phys. Rev. Lett. 86 (2001) 3200.
[4] C. Moore, M.E.J. Newman, Phys. Rev. E 61 (2000) 5678.
[5] L.A.N. Amaral, J.M. Ottino, Eur. Phys. J. B 38 (2) (2004) 147–162.
[6] D. Achlioptas, R.M. D'Souza, J. Spencer, Science 323 (2009) 1453.
[7] E.J. Friedman, A.S. Landsberg, Phys. Rev. Lett. 103 (2009) 255701.
[8] H.D. Rozenfeld, L.K. Gallos, H.A. Makse, Eur. Phys. J. B 75 (2010) 305.
[9] Y.S. Cho, J.S. Kim, J. Park, B. Kahng, D. Kim, Phys. Rev. Lett. 103 (2009) 135702.
[10] F. Radicchi, S. Fortunato, Phys. Rev. Lett. 103 (2009) 168701.
[11] R.M. D'Souza, M. Mitzenmacher, Phys. Rev. Lett. 104 (2010) 195702.
[12] R.M. Ziff, Phys. Rev. Lett. 103 (2009) 045701.
[13] R.M. Ziff, Phys. Rev. E 82 (2010) 051105.
[14] O. Riordan, L. Warnke, Science 333 (2011) 322.
[15] R.A. da Costa, S.N. Dorogovtsev, A.V. Goltsev, J.F.F. Mendes, Phys. Rev. Lett. 105 (2010) 255701.
[16] P. Grassberger, C. Christensen, G. Bizhani, S.-W. Son, M. Paczuski, Phys. Rev. Lett. 106 (2011) 225701.
[17] H.K. Lee, B.J. Kim, H. Park, Phys. Rev. E 84 (2011) 020101(R).
[18] L. Tian, D.-N. Shi, Phys. Lett. A 376 (2012) 286.
[19] M.X. Liu, J.F. Fan, L.S. Li, X.S. Chen, Eur. Phys. J. B 85 (4) (2012) 132.
[20] S.S. Manna, A. Chatterjee, Physica A 390 (2011) 177.
[21] S.S. Manna, Physica A 391 (2012) 2833.
[22] C. Christensen, G. Bizhani, S.-W. Son, M. Paczuski, P. Grassberger, Europhys. Lett. 97 (2012) 16004.
[23] J.S. Andrade Jr., H.J. Herrmann, A.A. Moreira, C.L.N. Oliveira, Phys. Rev. E 83 (2011) 031133.
[24] A.A. Moreira, E.A. Oliveira, S.D.S. Reis, H.J. Herrmann, J.S. Andrade Jr., Phys. Rev. E 81 (2010) 040101(R).
[25] N.A.M. Araújo, J.S. Andrade Jr., R.M. Ziff, H.J. Herrmann, Phys. Rev. Lett. 106 (2011) 095703.
[26] K.J. Schrenk, N.A.M. Araújo, H.J. Herrmann, Phys. Rev. E 84 (2011) 041136.
[27] S. Boettcher, V. Singh, R.M. Ziff, Nat. Commun. 3 (2012) 787.
[28] N.A.M. Araújo, H.J. Herrmann, Phys. Rev. Lett. 105 (2010) 035701.
[29] T. Bohman, A. Frieze, N.C. Wormald, Random Structures Algorithms 25 (2004) 432.
[30] W. Chen, R.M. D'Souza, Phys. Rev. Lett. 106 (2011) 115701.
[31] W. Chen, R.M. D'Souza, arXiv:1106.2088.
[32] K.J. Schrenk, A. Felder, S. Deflorin, N.A.M. Araújo, R.M. D'Souza, H.J. Herrmann, Phys. Rev. E 85 (2012) 031103.
[33] P.J. Reynolds, H.E. Stanley, W. Klein, J. Phys. A: Math. Gen. 10 (1977) L203–L209.
[34] M.E.J. Newman, I. Jensen, R.M. Ziff, Phys. Rev. E 65 (2002) 021904.
[35] A.-L. Barabasi, R. Albert, H. Jeong, Physica A 272 (1999) 173.
[36] J. Nagler, A. Levina, M. Timme, Nat. Phys. 7 (2011) 265.
[37] M.E.J. Newman, S.H. Strogatz, D.J. Watts, Phys. Rev. E 64 (2001) 026118.
[38] S.D.S. Reis, A.A. Moreira, J.S. Andrade, Phys. Rev. E 85 (2012) 041112.